
Gated Deep Neural Networks for Implied Volatility Surfaces

Yu Zheng^{b *} Yongxin Yang^{b †} Bowei Chen^{# ‡}

^b Department of Finance, Southwestern University of Finance and Economics, China

^b Department of Electrical and Electronic Engineering, University of Surrey, UK

[#] Adam Smith Business School, University of Glasgow, UK

Abstract

In this paper, we propose a gated deep neural network model to predict implied volatility surfaces. Conventional financial conditions and empirical evidence related to the implied volatility are incorporated into the neural network architecture design and calibration including no static arbitrage, boundaries, asymptotic slope and volatility smile. They are also satisfied empirically by the option data on the S&P 500 over a ten years period. Our proposed model outperforms the widely used surface stochastic volatility inspired model on the mean average percentage error in both in-sample and out-of-sample datasets. The research of this study has a fundamental methodological contribution to the emerging trend of applying the state-of-the-art information technology into business studies as our model provides a framework of integrating data-driven machine learning algorithms with financial theories and this framework can be easily extended and applied to solve other problems in finance or other business fields.

1 Introduction

Technology has been widely used in finance to bring automation and improve services. It includes using mobile phones for online banking, creating new digital assets like cryptocurrency, and developing data-driven machine learning algorithms for asset pricing and investment. These activities have formed an emerging new multidisciplinary field called *financial technology* (in short *fintech*). According to a recent report from [Ernst and Young \(2018\)](#), global fintech funding has a compound annual growth rate of 44% from 2013 to 2017. It increased in 2017 with US\$ 12.2 billion in the first three quarters as compared with US\$ 11.7 billion in the first three quarters of 2016. Within fintech, machine learning (or broadly artificial intelligence) has become one of the hottest sectors,

with expected direct investment growth of 63% from 2016 to 2022. In this paper, we investigate an application of the state-of-the-art machine learning in fintech – developing a new deep neural network for predicting implied volatility surfaces.

The research topic of our study in finance can be tracked back to the seminal work of [Black and Scholes \(1973\)](#). They proposed an option pricing model in which an underlying asset price is driven by a geometric Brownian motion containing a drift and a volatility where the volatility term shows small fluctuations of the asset returns representing risk. The study of volatility has become central to finance since the crash of 1987 ([Friz and Gatheral, 2005](#)). Specifically, the *implied volatility* of an option is defined as the inverse problem of option pricing, mapping from the option price in the current market to a single value ([Cont and Da Fonseca, 2002](#)). When it is plotted against the option strike price and the time to maturity, it is referred to as the *implied volatility surface*.

The methodologies of modelling implied volatility surfaces can be classified into two main groups ([Homescu, 2011](#)). The first group is called *indirect methods*, in which an implied volatility is driven by another dynamic model such as local volatility models, stochastic volatility models and Lévy models. Notable studies include [Merton \(1976\)](#), [Heston \(1993\)](#) and [Kou \(2002\)](#). Models in this group usually have a limited number of parameters, and the volatility term is fitted by the market data along with the asset dynamics. These models are sometimes invalid empirically though they exhibit mathematical elegance. Time-dependent parameters can be included, but this will greatly increase computational time and optimisation difficulty. The second group is called *direct methods*, in which an implied volatility is specified explicitly. Direct methods can also be divided into two types. The first type specifies the dynamics of an implied volatility surface and assumes it evolves continuously over time ([Cont and Da Fonseca, 2002](#); [Carr and Wu, 2010](#)). The second type pays attention to the static representation of implied volatility surfaces. It does not consider the evolution of the underlying asset, but uses either parametric or nonparametric methods to fit an implied volatility surface. Static models have been widely used by practitioners as they are able to provide a snapshot of the current market situation and usually fit the market data well.

One of the most popular static models is the stochastic volatil-

* ✉ zhengyu@swufe.edu.cn

† ✉ yongxin.yang@surrey.ac.uk

‡ ✉ bowei.chen@glasgow.ac.uk (corresponding author)

ity inspired (SVI) model proposed by Gatheral (2004). It models the implied volatility slice for a fixed time to maturity. Kotzé et al. (2013) then constructed an arbitrage-free implied volatility surface by introducing a quadratic deterministic volatility function, and the arbitrage-free conditions are forced by solving two minimization problems. Gatheral and Jacquier (2014) further updated the SVI model to the surface SVI (SSVI) model, which has simpler representations than the SVI on no static arbitrage conditions and has soon been widely adopted by investors. In addition, Itkin (2015) proposed a nonparametric method to model implied volatility surfaces using polynomials of sigmoid functions. However, arbitrage-free conditions are held only at the nodes of discrete strike-expiry space. Corlay (2016) employed B-splines to construct an arbitrage-free implied volatility surface and proposed a new calibration method tailored to sparse option data.

Machine learning in asset pricing and investment goes back more than a decade earlier, to the late 1980's or early 1990's. Malliaris and Salchenberger (1993) demonstrated that a single hidden layer neural network can offer a valuable alternative to estimating option prices to the traditional Black-Scholes model. Malliaris and Salchenberger (1996) then used several single hidden layer neural networks to forecast the future volatility of the S&P 100. Gavrishchaka (2006) proposed a boosting-based framework for volatility prediction in which a collection of generalized autoregressive conditional heteroskedasticity models are trained separately and then combined to form a strong predictor. This approach is also called *ensemble learning*. Audrino and Colangelo (2010) presented a semiparametric method for implied volatility surfaces in which the base model is a regression tree and the difference between the model prediction and the actual value is sequentially minimized by adding more trees. Coleman et al. (2013) used kernel machines (Vapnik, 2000) to calibrate the volatility function for option pricing. However, these studies only examined small datasets – Gavrishchaka (2006) targeted IBM stock options only, and Audrino and Colangelo (2010) and Coleman et al. (2013) worked on one-month data of the S&P 500 index options. Yang et al. (2017) proposed a class of gated neural networks that can automatically learn to divide-and-conquer the problem space (Gradojevic et al., 2009) for robust and accurate pricing European options.

Inspired by the work of Yang et al. (2017), we develop a gated neural network to predict implied volatility surfaces in this paper. Unlike many previous studies in which machine learning algorithms were used directly as a “black box”, our model is tailored to implied volatility surfaces. We design and calibrate the neural network by incorporating the related financial conditions and empirical evidence such as no static arbitrage, boundaries, asymptotic slope and volatility smile. Therefore, these heuristics should be met. From a high level perspective, our study bridges the gap between the data-driven machine learning algorithms and the existing financial theories. We develop a methodological framework to integrate both fields simultaneously, which can be applied to solve other problems in finance or other business fields. In addition, we validate the

proposed model with the option data on the S&P 500 over 10 years and also examine the options with a short time to maturity. Compared with related studies, our experimental setting is more challenging because it requires the model to be more robust and stable. In experiments, conventional financial conditions and empirical evidence are met empirically, and our model outperforms the widely used SSVI model on the mean average percentage error in both in-sample and out-of-sample datasets. It also outperforms other similar neural network models without incorporating financial conditions and empirical evidence, which further justifies the importance of integrating financial theories in model development.

The remainder of the paper is organised as follows: Section 2 introduces the mathematical preliminaries of neural networks; Section 3 introduces our proposed neural network model; Section 4 presents our experimental results; and Section 5 concludes the paper.

2 Neural Network Preliminaries

Neural networks (also called *connectionist systems* or *representation learning*) are a special machine learning or information processing paradigm that is inspired by ideas from psychology and neuroscience (Schmidhuber, 2015; Lecun et al., 2015). Simply, a neural network is a set of algorithms, modelled loosely after the human brain, that is designed to recognise patterns in data. Unlike conventional machine learning techniques, which are limited in their ability to process natural data in their raw form and require careful engineering and considerable domain expertise, neural networks allow a machine to be fed with raw data and can automatically discover the needed data representations for pattern recognition such as detection and classification. In other words, neural networks can learn and recognize patterns from data by examples, generally without being programmed with any task-specific rules from domain knowledge. For example, in image recognition, a neural network can learn to identify images that contain dogs by analyzing example images that have been manually labeled as “dog” or “not a dog” and using these to identify dogs in other images. They can automatically generate identifying characteristics from the raw data that they process without any prior knowledge about dogs. Therefore, neural networks are representation learning methods with multiple levels of representation, obtained by composing simple but non-linear modules that each transforms the representation at one level (starting with the raw input) into a representation at a higher, slightly more abstract level (Lecun et al., 2015). It is also widely believed that a neural network can approximate any continuous functions through different architecture designs of representation layers. This is known as the universal approximation theorem (Cybenko, 1989; Hornik, 1991).

The simplest neural network architecture contains two representation layers: an input layer where the data flows in, and an output layer where the predictions are produced. Suppose that the input data is of N -dimension, and the output is of M -dimension, a two-layer neural network can be expressed as

follows:

$$\hat{y} = x^T W + b, \quad (1)$$

where W is a matrix of size $N \times M$ and b is a vector of length M . In the literature of neural network, W is usually referred to as *weight term*, and b as *bias term*. Let Θ be a set of parameters where $\Theta = \{W, b\}$, the process of training a neural network (a.k.a. model calibration or parameter estimation) is to solve the following optimisation problem:

$$\operatorname{argmin}_{\Theta} \frac{1}{N} \sum_{n=1}^N \ell(y_n, \hat{y}_n) = \operatorname{argmin}_{W, b} \frac{1}{N} \sum_{n=1}^N \ell(y_n, x_n^T W + b), \quad (2)$$

where $\{x_n, y_n\}_{n=1,2,\dots,N}$ is called the *training data* and $\ell(y, \hat{y})$ is called the *loss function* which measures the difference between the ground-truth in data y and the model predictions \hat{y} , e.g., $\ell(y, \hat{y}) = (y - \hat{y})^2$ calculates the squared difference of two values.

The advanced neural network models are different to Eq. (1) from two architecture design settings: (i) the hidden layer; and (ii) the activation function. The hidden layer is an extra degree of computation. For example, a three-layer neural network can be written as follows:

$$\hat{y} = (x^T \bar{W} + \bar{b}) \tilde{W} + \tilde{b}, \quad (3)$$

where $\bar{W}, \bar{b}, \tilde{W}, \tilde{b}$ are matrices with dimensions $N \times K, K \times 1, K \times M, M \times 1$, respectively. Here K is a hyper-parameter¹ that indicates how many neurons in the hidden layer and we could simply denote $\Theta = \{\bar{W}, \bar{b}, \tilde{W}, \tilde{b}\}$. If a neural network with more than one hidden layer, it is called a deep neural network.

Activation functions can add non-linearity to the neural network. For example, we can add a sigmoid function into Eq. (3) for the hidden layer, and then it becomes

$$\hat{y} = \sigma(x^T \bar{W} + \bar{b}) \tilde{W} + \tilde{b}, \quad (4)$$

where $\sigma(\cdot)$ is the sigmoid function. Activation functions can be classified into two classes. The first class is the *scalar function*, which acts on neurons in an element-wise fashion so that the neurons do not affect each other. The common choices are the sigmoid function, the hyperbolic tangent function, the softplus function, and the rectified linear unit (ReLU) function. The second class is the vector function, which treats neurons as a vector, thus the value of one neuron may affect others. A common choice is the softmax function.

There is no unique receipt for developing a neural network. In following we briefly introduce some useful techniques to give a hint on how to design a neural network to solve financial problems. Inspired by Yang et al. (2017), financial conditions, assumptions or empirical evidence can be incorporated into neural network through activation functions, the weight constraint, the pseudo training data and the loss function. For

example, if a two-layer neural network needs to ensure its outputs to be positive values, we can slightly change its activation function and weight constraint as follows:

$$\hat{y} = \sigma(x^T \bar{W} + \bar{b}) e^{\tilde{W}} + e^{\tilde{b}}, \quad (5)$$

where $\sigma(\cdot)$ can be either the sigmoid function or the softplus function as both functions always produce positive values. If the neural network outputs need to be monotonically increasing or decreasing with respect to one of the input variable x , e.g., $\frac{\partial \hat{y}}{\partial x} > 0$ or $\frac{\partial \hat{y}}{\partial x} < 0$, we can the rewrite it as follows:

$$\hat{y} = \begin{cases} \sigma(xe^{\bar{W}} + \bar{b})e^{\tilde{W}} + \tilde{b}, & \text{if } \frac{\partial \hat{y}}{\partial x} > 0, \\ \sigma(-xe^{\bar{W}} + \bar{b})e^{\tilde{W}} + \tilde{b}, & \text{if } \frac{\partial \hat{y}}{\partial x} < 0. \end{cases} \quad (6)$$

Generating a set of pseudo data that softly constrain the function is proposed by Abu-Mostafa (1993). For example, if we want the function to be monotonically increase (e.g., a cumulative distribution function), we can generate N pseudo data and place the following loss function:

$$\ell = \sum_{n=1}^N \max(0, \hat{y}(x) - \hat{y}(x + \epsilon)), \quad (7)$$

where ϵ is a small positive values, e.g., 0.001. We can tell that the violation of monotonic increase property, e.g., $\hat{y}(x) > \hat{y}(x + \epsilon)$ for some generated x values, will lead to some loss. Thus the objective of optimisation will tend to find an appropriate function that has such property. The advantage of this approach is that it is very flexible; however, the property satisfaction needs to be double checked empirically. The constraints of financial problems can be incorporated into neural network by properly defining a loss function based on some pseudo training data. We will explain this in detail in Section 3.

3 Model

Let $(S_t)_{t \geq 0}$ be the spot price of an asset at time t , defined on a filtered probability space $(\Omega, \mathcal{F}, (\mathcal{F}_t)_{t \geq 0}, \mathbb{P})$, where Ω is the sample space, \mathcal{F} is a sigma-field, $(\mathcal{F}_t)_{t \geq 0}$ is a filtration and \mathbb{P} is the probability space. The market is assumed to be arbitrage-free and the time to maturity of a financial product is always finite. To avoid dealing with interest rates and dividends, the forward measure is used (Cont and Da Fonseca, 2002). Let $(F_{t,T})_{t \geq 0}$ be the forward price of the asset with maturity date T . Then $F_{t,T} := \frac{S_t}{B(t,T)}$ where $B(t,T)$ is the price at time t of a zero-coupon bond paying one unit at time T . The no-arbitrage assumption ensures there exists an equivalent martingale measure in which $(F_{t,T})_{t \geq 0}$ is a martingale. The log forward moneyness m can be obtained as $\log\{\frac{K}{F_{t,T}}\}$, where K is the strike price, and the annualized time to maturity τ is defined as $\frac{T-t}{A}$, where A is the annualization factor. Then the implied volatility $v(m, \tau)$ can be rewritten as a function of m and τ , the value of which can be obtained by inverting the BlackScholes option pricing formula (Black and Scholes, 1973).

¹Hyper-parameter is not learned through training data, but assigned before training.

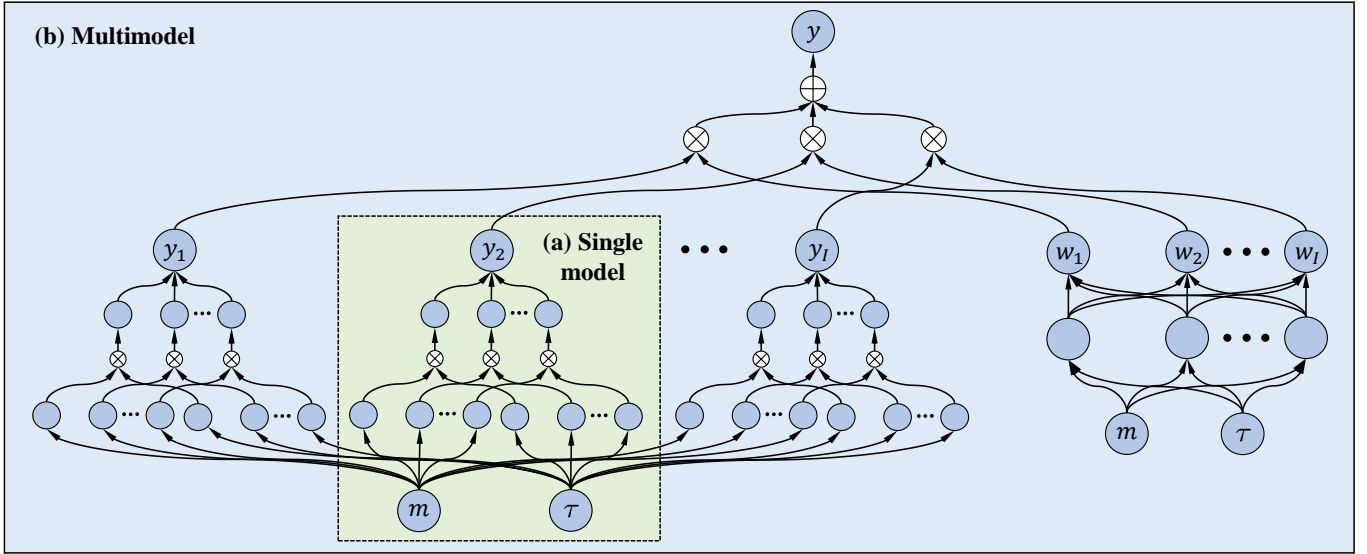


Figure 1: Schematic view of neural network architecture design: (a) the single model; (b) the multimodel. The multimodel consists of several single models and their weights are given by another neural network. Bias terms are omitted; \otimes is the multiplication gate operator; \oplus is the addition gate operator.

3.1 Setup

Implied volatility surfaces have been well studied in the financial literature. Theorem 1 presents the conditions for an implied volatility surface, in which conditions 1-5 ensure the absence of arbitrage (Gulisashvili, 2012); conditions 6-7 specify the boundaries (Carr and Wu, 2007); and condition 8 describes the log forward moneyness behavior (Lee, 2004).

Theorem 1 Let $d_{\pm}(m, \tau) = -\frac{m}{\sqrt{\tau}v(m, \tau)} \pm \frac{\sqrt{\tau}v(m, \tau)}{2}$, $n(\cdot)$ and $N(\cdot)$ be the probability density and cumulative functions of a standard normal distribution, respectively. The following conditions should hold for an implied volatility surface $v(m, \tau)$:

1. **(Positivity)** $v(m, \tau) > 0$ for all $(m, \tau) \in \mathbb{R} \times \mathbb{R}^+$.
2. **(Twice Differentiability)** For every $\tau > 0$, $m \rightarrow v(m, \tau)$ is twice differentiable on \mathbb{R} .
3. **(Monotonicity)** For every $m \in \mathbb{R}$, $\tau \rightarrow \sqrt{\tau}v(m, \tau)$ is increasing on \mathbb{R}^+ , therefore

$$v(m, \tau) + 2\tau\partial_{\tau}v(m, \tau) \geq 0.$$

4. **(Absence of Butterfly Arbitrage)** For all $(m, \tau) \in \mathbb{R} \times \mathbb{R}^+$,

$$\left(1 - \frac{m\partial_m v(m, \tau)}{v(m, \tau)}\right)^2 - \frac{(v(m, \tau)\tau\partial_m v(m, \tau))^2}{4} + \tau v(m, \tau)\partial_{mm}v(m, \tau) \geq 0.$$

5. **(Limit Condition)** For every $\tau > 0$

$$\lim_{m \rightarrow +\infty} d_+(m, \tau) = -\infty.$$

6. **(Right Boundary)** If $m \geq 0$, then

$$N(d_-(m, \tau)) - \sqrt{\tau}\partial_m v(m, \tau)n(d_-(m, \tau)) \geq 0.$$

7. **(Left Boundary)** If $m < 0$, then

$$N(-d_-(m, \tau)) + \sqrt{\tau}\partial_m v(m, \tau)n(d_-(m, \tau)) \geq 0.$$

8. **(Asymptotic Slope)** For every $\tau > 0$,

$$2|m| - v^2(m, \tau)\tau > 0.$$

In addition to Theorem 1, volatility smile has been considered an important empirical evidence, which will be included in our model. Specifically, when the implied volatility is plotted against the strike price, it creates a line that slopes upward on either end, looking like a ‘‘smile’’. In order to include volatility smile in our model, the following smile function $\phi(\cdot)$ for the log forward moneyness is defined:

$$\phi(z) = \sqrt{\left(z \tanh\left(z + \frac{1}{2}\right) + \tanh\left(-\frac{1}{2}z + \epsilon\right)\right)^2}, \quad z \in \mathbb{R}, \quad (8)$$

where $\tanh(\cdot)$ is the hyperbolic tangent function and ϵ is a small value to ensure numerical stability. The function can exhibit not only a skew pattern like volatility smile, but also meets the second condition of Theorem 1 as it is smoothly twice differentiable with the codomain of $(0, \infty)$.

3.2 Architecture Design

Fig. 1 presents a schematic view of our neural network architecture design. Our model is called the *multimodel* because it uses several single models as building blocks and their weights are specified by another neural network. The input of the

multimodel is the log forward moneyness m and the time to maturity τ ; and the output is the predicted implied volatility $\hat{v}(m, \tau)$. Simply, a neural network is based on a collection of connected units called *neurons*. Each connection can transmit a signal from one neuron to another. In our design, additional arithmetic operations on signal transmission are performed at some stages in terms of gate operators. For example, \otimes is the multiplication gate operator that multiplies the signals it receives, and \oplus is the addition gate operator, which sums up the signals it receives. For the reader's convenience, a brief description of model parameters is given in Table 1. Please refer to Goodfellow et al. (2016) for the fundamentals of neural network architecture design.

As shown in Fig. 1, every single model can be used to model an implied volatility surface. Mathematically, a single model can be expressed as follows:

$$\begin{aligned}\hat{v}(m, \tau) &= y(m, \tau) \\ &= \sum_{j=1}^J \phi(m\bar{W}_{1,j} + \bar{b}_j) \psi(\tau\tilde{W}_{1,j} + \tilde{b}_j) e^{\hat{W}_{j,1}} + e^{\hat{b}},\end{aligned}\quad (9)$$

where $\phi(\cdot)$ is the smile function to activate neurons related to m and $\psi(\cdot)$ is the sigmoid function to activate neurons related to τ , J is the number of neurons in the hidden layer, and \bar{b} , \bar{W} , \tilde{b} , \tilde{W} , \hat{W} , \hat{b} are network parameters. Each of \bar{b} , \bar{W} , \tilde{b} , \tilde{W} , \hat{W} has J elements and \hat{b} has one element. Therefore, there is a total of $5J + 1$ parameter values. It should be noted that the predicted implied volatility from Eq. (9) is always positive, satisfying the first condition of Theorem 1. This is because the outputs of activation functions are nonnegative, and the weight and bias terms are embedded by exponential functions.

Here, we use single models as building blocks and combine them to construct a deeper and more complex architecture. Our multimodel can be expressed as follows:

$$\hat{v}(m, \tau) = \sum_{i=1}^I y_i(m, \tau) w_i(m, \tau), \quad (10)$$

$$y_i(m, \tau) = \sum_{j=1}^J \phi(m\bar{W}_{1,j}^{(i)} + \bar{b}_j^{(i)}) \psi(\tau\tilde{W}_{1,j}^{(i)} + \tilde{b}_j^{(i)}) e^{\hat{W}_{j,1}^{(i)}} + e^{\hat{b}^{(i)}}, \quad (11)$$

$$w_i(m, \tau) = \frac{e^{\Phi}}{\sum_{i=1}^I e^{\Phi}}, \quad (12)$$

$$\Phi = \sum_{k=1}^K \psi(m\dot{W}_{1,k} + \tau\dot{W}_{2,k} + \dot{b}_k) \ddot{W}_{k,i} + \ddot{b}_i, \quad (13)$$

where \dot{W} , \dot{b} , \ddot{W} , \ddot{b} are the newly added parameter terms of the network for weighting single models. The dimensions of \dot{W} , \dot{b} , \ddot{W} , \ddot{b} are $2 \times K$, $K \times 1$, $K \times I$, and $I \times 1$, respectively. Therefore, the total number of parameter values in the multimodel is $(5J + K + 2)I + 3K$.

3.3 Constrained Optimisation

The designed neural network needs to be calibrated with the market data so that it can be used for prediction. Such a process is called *model training* in the machine learning literature. The aim is to minimize the in-sample difference between the predicted \hat{v} and the v calculated by inverting the BlackScholes model. The latter is also called the *ground truth*. Mathematically, the model training can be expressed by minimizing a loss function ℓ as follows:

$$\min \ell = \ell_0 + \gamma \ell_1 + \delta \ell_2 + \eta \ell_3 + \rho \ell_4 + \omega \ell_5, \quad (14)$$

$$\begin{aligned}\ell_0 &= \alpha \underbrace{\left(\frac{1}{N} \sum_{n=1}^N (\log(v_n) - \log(\hat{v}_n))^2 \right)}_{\text{MSLE}} \\ &\quad + \beta \underbrace{\left(\frac{1}{N} \sum_{n=1}^N \left(\frac{v_n - \hat{v}_n}{v_n} \right)^2 \right)}_{\text{MSPE}},\end{aligned}\quad (15)$$

$$\ell_1 = \sum_{p=1}^P \sum_{q=1}^Q \max(0, -a(m_p, \tau_q)), \quad (16)$$

$$\ell_2 = \sum_{p=1}^P \sum_{q=1}^Q \max(0, -b(m_p, \tau_q)), \quad (17)$$

$$\begin{aligned}\ell_3 &= \sum_{p_1=1}^{P_1} \sum_{q=1}^Q \max(0, -c_1(m_{p_1}, \tau_q)) \\ &\quad + \sum_{p_2=1}^{P_2} \sum_{q=1}^Q \max(0, -c_2(m_{p_2}, \tau_q)),\end{aligned}\quad (18)$$

$$\ell_4 = \sum_{p=1}^P \sum_{q=1}^Q \max(0, -(g(m_p, \tau_q) - \epsilon)), \quad (19)$$

$$\ell_5 = \begin{cases} \|\bar{W}\|_F^2 + \|\tilde{W}\|_F^2 + \|\hat{W}\|_F^2, & \text{single model,} \\ \sum_{i=1}^I \|\bar{W}^{(i)}\|_F^2 \\ + \sum_{i=1}^I \|\tilde{W}^{(i)}\|_F^2 \\ + \sum_{i=1}^I \|\hat{W}^{(i)}\|_F^2 \\ + \|\dot{W}\|_F^2 + \|\ddot{W}\|_F^2, & \text{multimodel.} \end{cases}\quad (20)$$

where ℓ_0 represents the data loss, ℓ_1, \dots, ℓ_4 are the loss functions that incorporate financial conditions discussed in Theorem 1, ℓ_5 is the regularization term to avoid overfitting, and $\gamma, \delta, \eta, \rho, \omega$ are hyperparameters controlling the weights.

Specifically, ℓ_0 is a joint loss – it is a sum of the mean squared log error (MSLE) and the mean squared percentage error (MSPE), where α and β are hyperparameters to control their weights. In machine learning, a joint loss is often used to deal with sensitive data or high-dimensional feature spaces (Goodfellow et al., 2016). ℓ_1 specifies the monotonicity condition where $a(m, \tau) := v(m, \tau) + 2\tau \partial_\tau v(m, \tau)$ and the objective is to push $a(m, \tau)$ to be nonnegative. This can be achieved by randomly sampling P unique values from the domain of m and Q unique values from the domain of τ . It is not

Table 1: Summary of neural network parameters.

Notation	Description	Shape	Number in single model	Number in multimodel
\bar{W}	Weight term for moneyness	$1 \times J$	1	I
\bar{b}	Bias term for moneyness	$J \times 1$	1	I
$\tilde{\bar{W}}$	Weight term for time to maturity	$1 \times J$	1	I
$\tilde{\bar{b}}$	Bias term for time to maturity	$J \times 1$	1	I
\hat{W}	Weight term for final pricing	$J \times 1$	1	I
\hat{b}	Bias term for final pricing	1	1	I
\dot{W}	Weight term for weighting model hidden	$2 \times K$	0	1
\dot{b}	Bias term for weighting model hidden	$K \times 1$	0	1
\ddot{W}	Weight term for weighting model output	$K \times I$	0	1
\ddot{b}	Bias term for weighting model output	$I \times 1$	0	1

difficult to see that ℓ_1 adds a penalty if negative values are produced by $a(m, \tau)$ for a certain set of (m, τ) pairs. Therefore, if an infinite number of samples is generated, ℓ_1 can be reduced to zero during the optimisation and the condition would be met. ℓ_2 specifies the absence of a butterfly arbitrage condition where $b(m, \tau) := (1 - \frac{m\partial_m v(m, \tau)}{v(m, \tau)})^2 - \frac{(v(m, \tau)\tau\partial_m v(m, \tau))^2}{4} + \tau v(m, \tau)\partial_{mm} v(m, \tau)$ and the objective is to push $b(m, \tau)$ to be nonnegative. This can be achieved using the same way as ℓ_1 , by randomly sampling P unique values from the domain of m and Q unique values from the domain of τ . ℓ_3 specifies the left and right boundary conditions where $c_1(m, \tau) := N(d_-(m, \tau)) - \sqrt{\tau}\partial_m v(m, \tau)n(d_-(m, \tau))$ and $c_2(m, \tau) := N(-d_-(m, \tau)) + \sqrt{\tau}\partial_m v(m, \tau)n(d_-(m, \tau))$. The objective is to push both functions to be nonnegative. To achieve this, we sample P_1 unique nonnegative values from the domain of m , P_2 unique negative values from the domain of m and Q unique values from the domain of τ . ℓ_4 specifies the asymptotic condition where $g(m, \tau) := 2|m| - v^2(m, \tau)\tau$ and ϵ is a very small value, which ensures $g(m, \tau)$ will be positive. So, we sample P unique values from the domain of m and Q unique values from the domain of τ . It is worth mentioning that the values of m and τ in ℓ_1, \dots, ℓ_4 can also be sampled from the training data. However, the calibrated neural network may fail to meet those conditions when the given values of m and τ for prediction are out of the scope of the training data. In machine learning, if the training data have limited observations of input variables, creating synthetic data by sampling values from their domains is often used in model training (Choe et al., 2017; Liu et al., 2017). Finally, the regularization term ℓ_5 is a linear combination of squared Frobenius norms, which is denoted by $\|\cdot\|_F^2$.

4 Experiments

In this section, we describe our option data, explain the experimental settings, present and discuss our experimental results.

4.1 Data

Our option data on the S&P 500 are obtained from OptionMetrics. They include a total of 5,116 trading days, cover-

ing the period from 04/01/1996 to 29/04/2016. OptionMetrics also provides data on the zero-coupon yield curve, which is constructed based on the London Inter-bank Offered Rate (LIBOR). However, because the traditional LIBOR-based zero curve is not risk-free after the 2008 financial crisis (Ametrano and Bianchetti, 2013), we extract the Overnight Index Swap (OIS) rates from Bloomberg and bootstrap the zero rate curve from the OIS for the period from 01/01/2008 to 14/10/2016. The zero rate curve provided by OptionMetrics is used for the data prior to 01/01/2008. The risk-free rates are interpolated using a cubic spline to match the option maturity. Forward price is estimated by the put-call parity (Bilson et al., 2015).

4.2 Experimental Settings

The original option data are further filtered before model training. Option quotes of less than 3/8 are excluded because they are close to tick size, which might be misleading. Bid-ask mid-point price is calculated as a proxy for closing price. In-the-money option quotes are excluded because of small transaction volume (Bliss and Panigirtzoglou, 2005). Scholars usually do not analyze option contracts with time to maturity of less than 7 days (Andersen et al., 2017). However, as these options are getting popular recently, e.g., weekly index options, we here analyze option contracts with a short time to maturity and only exclude the contracts with maturity of less than 2 days. Analyzing options with a short time to maturity is challenging because it requires a model with high robustness and stability. The finally selected data contain 63,338 option contracts with 2,986,754 valid quotes. The quotes are then used to calculate implied volatility values by inverting the BlackScholes option pricing formula.

Fig. 2 provides a descriptive summary of the selected data. As shown in Fig. 2(a), the number of option contracts doubled from 2007 to 2012, and it reached more than 30 contracts for each day in 2016. Therefore, in Fig. 2(b), the number of quotes increases exponentially. Fig. 2(c)(d) present the range of the time to maturity and the log moneyness, which are $[1, 3]$ and $[-3, 1]$, respectively. By incorporating financial conditions and empirical evidence (as well as generating synthetic data in constrained optimisation in Section 3.3), the trained

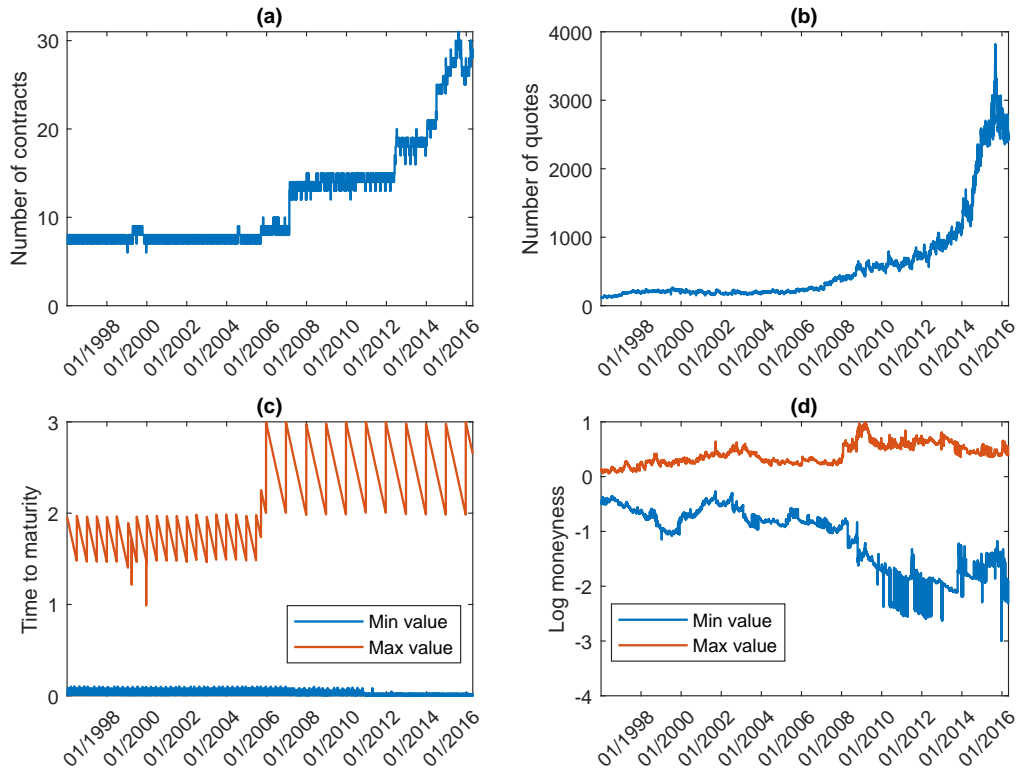


Figure 2: Time series plots of options from 04/01/1996 to 29/04/2016: (a) the number of contracts; (b) the number of quotes; (c) the time to maturity; (d) the log moneyness.

Table 2: Experimental settings of hyper parameters.

Parameter	Multi	Multi [†]	Single	Single [†]	Vanilla	Vanilla [†]
I	4	4	1	1	1	1
J	8	8	32	32	32	32
K	5	5	-	-	-	-
Initial learning rate	0.1	0.1	0.1	0.1	0.1	0.1
Number of iterations	20000	20000	20000	20000	20000	20000
α	1	1	1	1	1	1
β	1	1	1	1	1	1
γ	10	0	10	0	10	0
δ	1	0	1	0	1	0
η	10	0	10	0	10	0
ρ	1	0	1	0	1	0
ω	0.00005	0.00005	0.00005	0.00005	0.00005	0.00005

[†] Model with incomplete constraints.

Table 3: Mean and standard deviation (Std) of the MAPEs for all models.

Model	Implied volatility				Option price			
	Training set		Test set		Training set		Test set	
	Mean	Std	Mean	Std	Mean	Std	Mean	Std
Multi	1.74	0.50	3.34	2.18	5.97	1.86	10.64	6.72
Multi [†]	1.76	0.50	3.35	2.17	6.03	1.86	10.67	6.70
Single	2.15	0.67	3.60	2.12	7.38	2.57	11.64	6.68
Single [†]	1.82	0.52	3.38	2.16	6.20	1.91	10.77	6.67
Vanilla	3.21	0.98	4.46	2.07	11.31	3.57	14.61	6.42
Vanilla [†]	2.87	0.80	4.18	2.04	10.53	3.34	14.17	6.60
SSVI	2.59	0.85	3.73	2.18	8.71	2.72	12.74	6.74

[†] Model with incomplete constraints

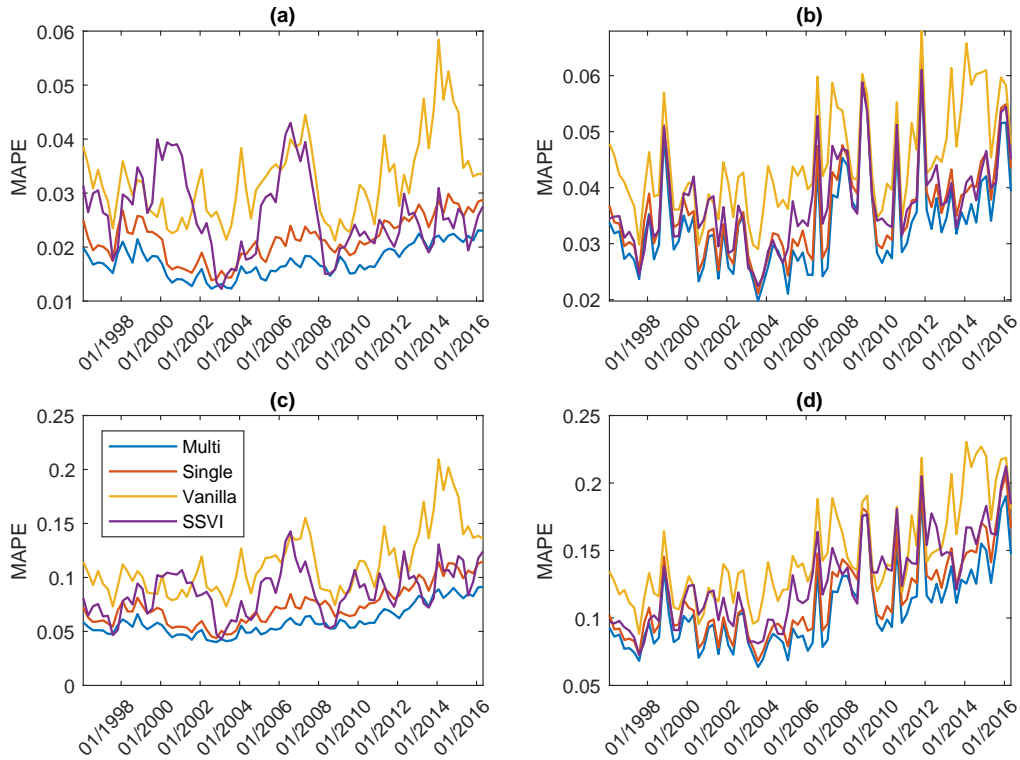


Figure 3: Plots of the MAPEs in each quarter for the neural network models and the SSVI of: (a) implied volatilities in the training set; (b) implied volatilities in the test set; (c) option prices in the training set; (d) option prices in the test set.

neural networks are then able to learn implied volatility surfaces outside those ranges.

Our model is the multimodel. It is compared with the single model and the SSVI for the benchmark. We also compare it with a neural network with the simplest architecture, which has a single hidden layer using the sigmoid activation function and only one constraint that ensures positive output. For simplicity, we call it the *vanilla model*. In addition, to justify the importance of embedding financial conditions in the constrained optimisation, all neural network models are further trained under a setting where ℓ_1, \dots, ℓ_4 are removed from the loss function in Eq. (14), called the *incomplete constraints* setting. Finally, seven models are examined in experiments, including six different versions of neural networks, the hyperparameter settings of which are summarized in Table 2. To avoid the effect of model size on model performance, neural networks with the same architecture design are specified with the same model size. Synthetic data are generated to meet the constraints specified by Eqs. (16)-(19). The ratio of real market data and synthetic data is 1/6. m is sampled in $[-6, -3] \cup [3, 6]$ for the asymptotic condition and in $[-3, 3]$ for other conditions; τ is sampled in $[0.002, 3]$. These values are set based on the observations from historical data, as shown in Fig. 2 (c)(d).

4.3 Results

Neural network models are trained using TensorFlow. We use the method proposed by Kingma and Ba (2015) for stochas-

tic optimisation. The selected option quotes available on each trading day are used to compute the mean average percentage error (MAPE) of implied volatilities. The latter can be used to compute option prices; therefore, the MAPE of option prices can be obtained. In the following, we compare our proposed model with the benchmarked models, check if the financial conditions are satisfied, and then investigate the effects of constraints in the optimisation.

Table 3 provides an overall summary of the mean and the standard deviation of MAPEs of implied volatility and option price for each examined model. Our proposed multimodel outperforms other models: (i) on both implied volatility and option price; and (ii) in both training and test sets. The training set result shows the in-sample error representing how good the model fits the data in calibration, while the test set result shows the out-of-sample error representing the prediction power of the model. Except for vanilla models, other neural network models achieve better performance than the widely used SSVI, affirming that our network architecture design has a great advantage of modelling implied volatility surfaces. Models with incomplete constraints are slightly behind the models with full constraints. Fig. 3 further plots the MAPEs of each quarter to compare the (complete) models with the SSVI in both training and test sets. The multimodel can dynamically capture the data patterns and has the smallest and the most stable moving MAPE over time.

Fig. 4 checks whether the financial conditions set in Theorem 1 are satisfied by neural network models over time, in-

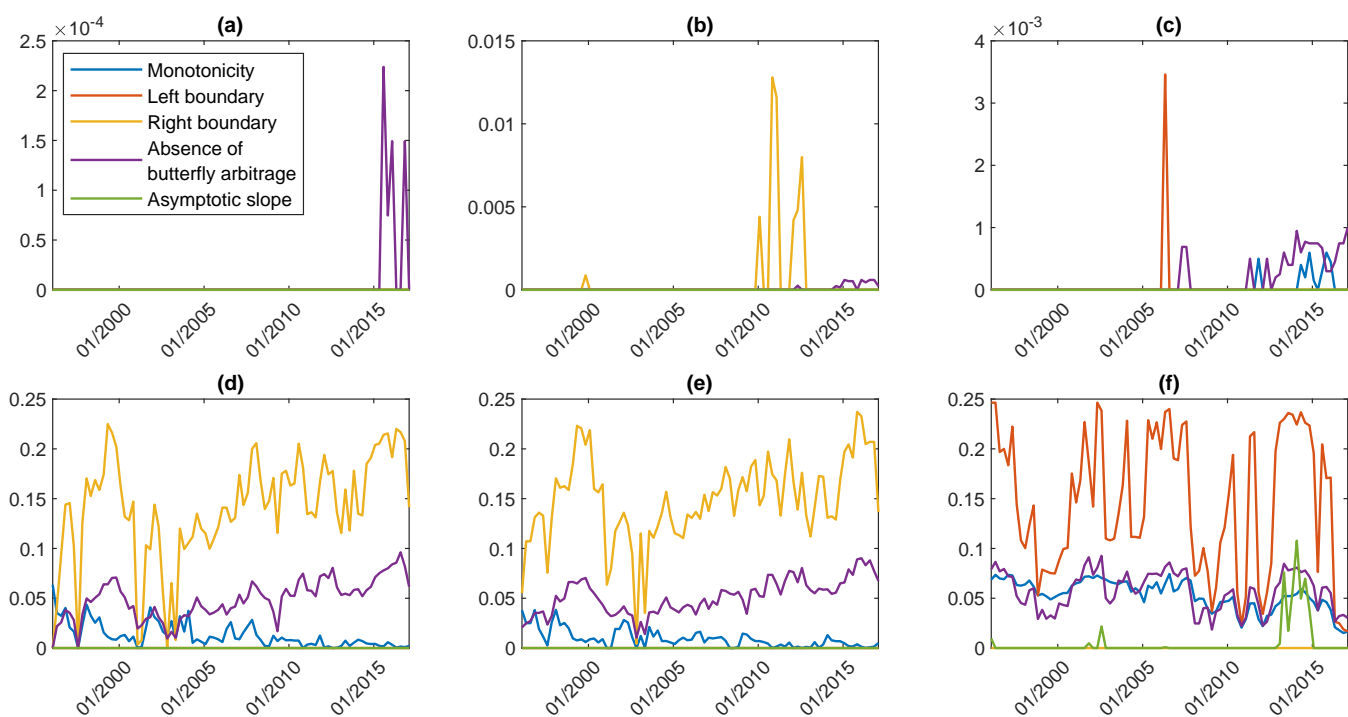


Figure 4: Plots of condition checks of: (a) the multimodel; (b) the single model; (c) the vanilla model; (d) the multimodel with incomplete constraints; (e) the single model with incomplete constraints; (f) the vanilla model with incomplete constraints.

cluding monotonicity, left boundary, right boundary, absence of arbitrage and asymptotic slope. These conditions are met by the multimodel because the violation percentages are less than 0.1%. Overall, the complete models are more robust than models with incomplete constraints. This confirms the importance and necessity of incorporating financial conditions. Figs. 5-6 show why regularization is needed, check if the limit condition is met and compare the implied volatility surface from the multimodel and the multimodel without regularization on 11/01/2016. As described earlier, regularization is usually used to avoid overfitting (Goodfellow et al., 2016), and we can see that the implied volatility surface generated by the multimodel without regularization is not smooth with the “smile” pattern (i.e., plotting v against m when τ is fixed). Fig. 6 further plots the risk-neutral density extracted from the multimodel and the multimodel without regularization for forward return with 11, 32, 109 and 704 days duration. The densities of the 109 and 704 days in the multimodel without regularization look strangely like a mixed model. Fig. 6(c) further verifies the limit condition because $d_+(m, \tau) \rightarrow -\infty$ if $m \rightarrow \infty$.

5 Conclusion

In this paper, a gated neural network model is designed to predict implied volatility surfaces. Unlike many previous studies where machine learning techniques were mainly used as a “black box” or were less connected with the existing financial theories, our model incorporates the related impor-

tant financial conditions and empirical evidence. To the best of our knowledge, this is one of very first studies which discuss a methodological framework that can integrate the data-driven machine learning algorithms (particularly deep neural networks) with the existing financial theories. The model framework can be easily extended and applied to solve other similar problems in fintech or other business fields. In addition to methodological contributions, we validate the proposed model empirically with the option data on the S&P 500. Compared with the existing studies, our experimental settings are more challenging as the used option data is over 10 years and the options with a short time to maturity are examined. In order to produce convincing results, our model needs to be more robust and stable. As presented in Section 4, conventional financial conditions and empirical evidence are met empirically; our model outperforms the widely used SSVI model; and it also outperforms other similar neural network models without incorporating financial conditions and empirical evidence. The last result also justifies the importance of integrating financial theories into the model.

Acknowledgement

This work was conducted with the support of the ESRC IAA Business Booster Fund.

References

Y. Abu-Mostafa. A method for learning from hints. *Neural Information Processing Systems*, 1993.

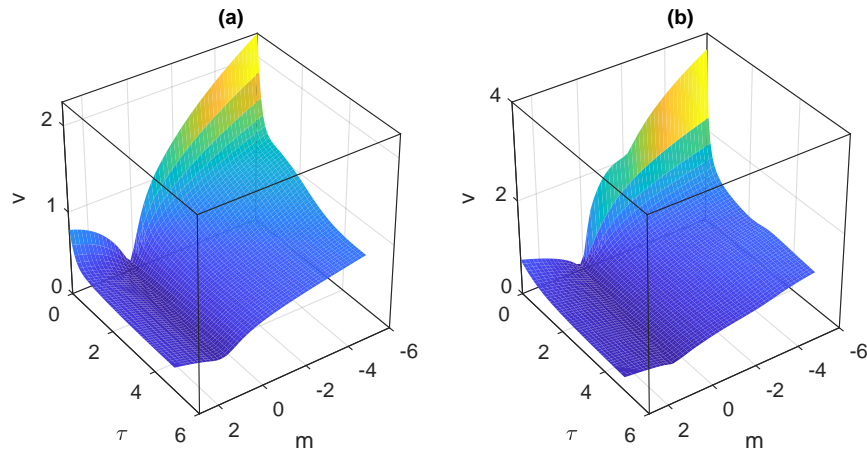


Figure 5: Plots the implied volatility surface on 11/01/2016 for: (a) the multimodel; and (b) the multimodel without regularization.

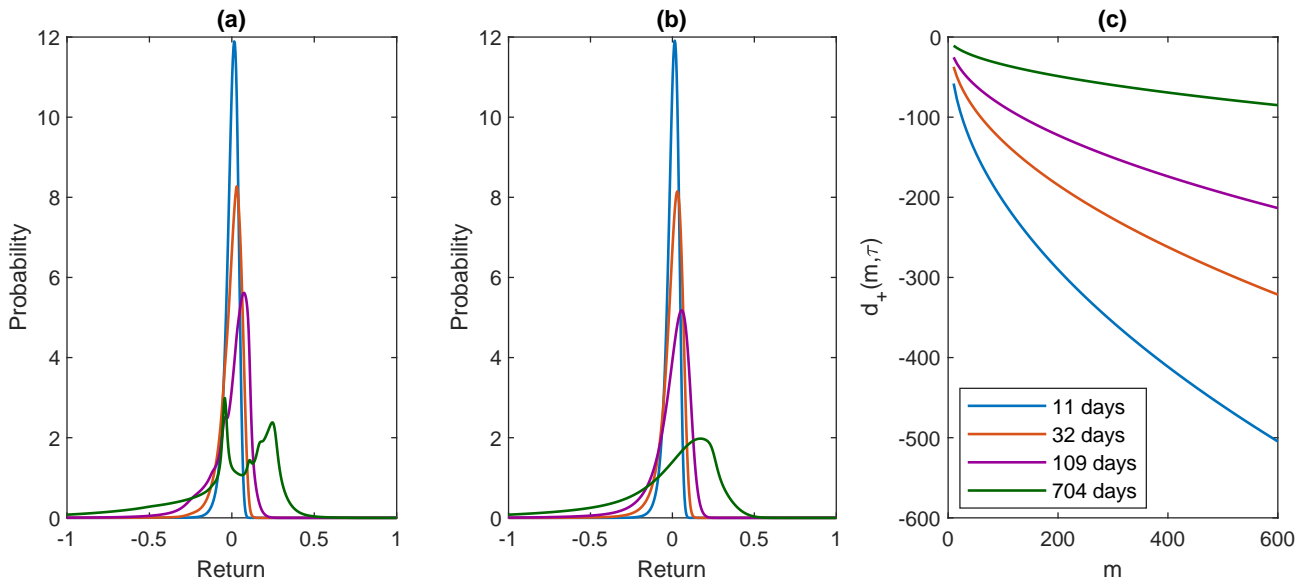


Figure 6: Plots for the forward with 11, 32, 109 and 704 days duration: (a) the density of returns from the multimodel without regularization; (b) the density of returns from the multimodel; and (c) the limit condition $d_+(m, \tau)$ in Theorem 1 for the multimodel on 11/01/2016.

F. Ametrano and M. Bianchetti. Everything you always wanted to know about multiple interest rate curve bootstrapping but were afraid to ask. SSRN, 2013. https://papers.ssrn.com/sol3/papers.cfm?abstract_id=2219548.

T. Andersen, N. Fusari, and V. Todorov. Short-term market risks implied by weekly options. *The Journal of Finance*, 72(3):1335–1386, 2017.

F. Audrino and D. Colangelo. Semi-parametric forecasts of the implied volatility surface using regression trees. *Statistics and Computing*, 20(4):421–434, 2010.

J. Bilson, S. Kang, and H. Luo. The term structure of implied dividend yields and expected returns. *Economics Letters*, 128:9–13, 2015.

F. Black and M. Scholes. The pricing of options and corporate liabilities. *Journal of Political Economy*, 81(3):637–654, 1973. ISSN 00223808.

R. Bliss and N. Panigirtzoglou. Option-implied risk aversion estimates. *The Journal of Finance*, 59(1):407–446, 2005.

P. Carr and L. Wu. Stochastic skew in currency options. *Journal of Financial Economics*, 86(1):213–247, 2007.

P. Carr and L. Wu. A new simple approach for constructing implied volatility surfaces. SSRN, 2010. https://papers.ssrn.com/sol3/papers.cfm?abstract_id=1701685.

J. Choe, S. Park, K. Kim, J. H. Park, D. Kim, and H. Shim. Face generation for low-shot learning using generative adversarial networks. *IEEE International Conference on Computer Vision Workshops*, pages 1940–1948, 2017.

- T. Coleman, Y. Li, and C. Wang. Stable local volatility function calibration using spline kernel. *Computational Optimization and Applications*, 55(3):675–702, 2013.
- R. Cont and J. Da Fonseca. Dynamics of implied volatility surfaces. *Quantitative Finance*, 2(1):45–60, 2002.
- S. Corlay. B-spline techniques for volatility modeling. *Journal of Computational Finance*, 19(3):97–135, 2016.
- G. Cybenko. Approximation by superpositions of a sigmoidal function. *Mathematics of Control, Signals and Systems*, 2(4):303–314, 1989. ISSN 1435-568X. doi: 10.1007/BF02551274. URL <http://dx.doi.org/10.1007/BF02551274>.
- Ernst and Young. The future of FinTech and financial services: whats the next big bet?, 2018.
- P. Friz and J. Gatheral. Valuation of volatility derivatives as an inverse problem. *Quantitative Finance*, 5(6):531–542, 2005.
- J. Gatheral. A parsimonious arbitrage-free implied volatility parameterization with application to the valuation of volatility derivatives. *Presentation at Global Derivatives & Risk Management*, Madrid, 2004.
- J. Gatheral and A. Jacquier. Arbitrage-free svi volatility surfaces. *Quantitative Finance*, 14(1):59–71, 2014.
- V. Gavrishchaka. *Econometric Analysis of Financial and Economic Time Series*, chapter Boosting-based Frameworks in financial modeling: application to symbolic volatility forecasting, pages 123–151. Emerald, 2006.
- I. Goodfellow, Y. Bengio, and A. Courville. *Deep Learning*. MIT Press, 2016.
- N. Gradojevic, R. Gencay, and D. Kukulj. Option pricing with modular neural networks. *IEEE Transactions on Neural Networks*, 20(4):626–637, 2009.
- A. Gulisashvili. *Analytically Tractable Stochastic Stock Price Models*. Springer, 2012.
- S. Heston. A closed-form solution for options with stochastic volatility with applications to bond and currency options. *Review of Financial Studies*, 6(2):327–343, 1993.
- C. Homescu. Implied volatility surface: construction methodologies and characteristics. arXiv, 2011. <https://arxiv.org/abs/1107.1834>.
- K. Hornik. Approximation capabilities of multilayer feed-forward networks. *Neural Netw.*, 4(2):251–257, Mar. 1991. ISSN 0893-6080. doi: 10.1016/0893-6080(91)90009-T. URL [http://dx.doi.org/10.1016/0893-6080\(91\)90009-T](http://dx.doi.org/10.1016/0893-6080(91)90009-T).
- A. Itkin. To sigmoid-based functional description of the volatility smile. *The North American Journal of Economics and Finance*, 31:264–291, 2015.
- D. Kingma and J. Ba. Adam: a method for stochastic optimization. *International Conference on Learning Representations*, pages 1–13, 2015.
- A. Kotzé, C. Labuschagne, M. Nair, and N. Padayachi. Arbitrage-free implied volatility surfaces for options on single stock futures. *The North American Journal of Economics and Finance*, 26:380–399, 2013.
- S. Kou. A jump-diffusion model for option pricing. *Management Science*, 48(8):1086–1101, 2002.
- Y. Lecun, Y. Bengio, and G. Hinton. Deep learning. *Nature*, 521(7553):436–444, 5 2015. ISSN 0028-0836. doi: 10.1038/nature14539.
- R. Lee. The moment formula for implied volatility at extreme strikes. *Mathematical Finance*, 14(3):469–480, 2004.
- T. Liu, Y. Cui, Q. Yin, W. Zhang, S. Wang, and G. Hu. Generating and exploiting large-scale pseudo training data for zero pronoun resolution. *Proceedings of the 55th Annual Meeting of the Association for Computational Linguistics*, pages 102–111, 2017.
- M. Malliaris and L. Salchenberger. A neural network model for estimating option prices. *Applied Intelligence*, 3(3):193–206, 1993.
- M. Malliaris and L. Salchenberger. Using neural networks to forecast the S&P 100 implied volatility. *Neurocomputing*, 10(2):183–195, 1996.
- R. Merton. Option pricing when underlying stock returns are discontinuous. *Journal of Financial Economics*, 3:125–144, 1976.
- J. Schmidhuber. Deep learning in neural networks: An overview. *Neural Networks*, 61:85–117, 2015.
- V. Vapnik. *The Nature of Statistical Learning Theory*. Springer, 2nd edition, 2000.
- Y. Yang, Y. Zheng, and T. Hospedales. Gated neural networks for option pricing: rationality by design. *Proceedings of the Thirty-First AAAI Conference on Artificial Intelligence*, 2017.